

As a library, NLM provides access to scientific literature. Inclusion in an NLM database does not imply endorsement of, or agreement with, the contents by NLM or the National Institutes of Health.

Learn more: [PMC Disclaimer](#) | [PMC Copyright Notice](#)

Author Manuscript

Peer reviewed and accepted for publication by a journal



[Exp Dermatol.](#) Author manuscript; available in PMC 2010 Oct 19.

PMCID: PMC2957116

Published in final edited form as:

NIHMSID: NIHMS239802

[Exp Dermatol. 2010 Aug; 19\(8\): e16–e22.](#)

PMID: [19650866](#)

doi: [10.1111/j.1600-0625.2009.00945.x](#)

Analysis of ionizing radiation-induced DNA damage and repair in three-dimensional human skin model system

[Yanrong Su](#), [Jarah A. Meador](#), [Charles R. Geard](#), and [Adayabalam S. Balajee](#)

Abstract

Knowledge of cellular responses in tissue microenvironment is crucial for the accurate prediction of human health risks following chronic or acute exposure to ionizing radiation (IR). With this objective, we investigated the radio responses for the first time in three-dimensional (3D) artificial human skin tissue microenvironment after γ -rays radiation. IR-induced DNA damage/repair response was assessed by immunological analysis of well-known DNA double strand break (DSB) repair proteins, i.e. 53BP1 and phosphorylated ataxia telangiectasia mutated^{ser1981} (ATM^{ser1981}). Efficient 53BP1 and phosphorylated ATM foci formation was observed in human EpiDerm tissue constructs after low and high doses of γ -rays. Interestingly, EpiDerm tissue constructs displayed less 53BP1 and ATM foci number at all radiation doses (0.1, 1, 2.5 and 5 Gy) than that observed for 2D human fibroblasts. DSB repair efficiency judged by the disappearance of 53BP1 foci declined with increasing doses of γ -rays and tissue constructs irradiated with 2.5 and 5 Gy of γ -rays displayed 53BP1 foci persisting up to 72 h of analysis. Pretreatment of EpiDerm tissue constructs with LY294002, [an inhibitor of phosphatidylinositol-3 kinase and PI-3 kinase like kinases (PIKK)] completely abolished IR-induced 53BP1 foci formation and increased the apoptotic death. This observation indicates the importance of PIKK signalling pathway for efficient radiation responses in intact tissue constructs. In summary, we have successfully demonstrated the

feasibility of monitoring the DNA damage response in human skin tissue microenvironment. In this system, 53BP1 can be used as a useful marker for monitoring the DSB repair efficiency.

Keywords: 53 binding protein 1, double strand break induction and repair, EpiDerm tissue constructs, low LET radiation, phosphatidylinositol-3 kinase like kinases

Introduction

Exposure to ionizing radiation (IR) inflicts single strand breaks, double strand breaks (DSB), base damage and DNA-protein cross-links in the genomic DNA. Among them, DSB is the most critical lesion, which when misre-paired or unrepaired, can lead to genomic instability and cell death. Two major DSB repair pathways, non-homologous end joining (NHEJ) and homologous recombination repair (HRR), operate in eukaryotic cells. Some important players in NHEJ include DNA ligase IV/XRCC4 (X-ray cross complementation group 4) DNA-dependent protein kinase (DNA-PK), Ku70 and Ku80. In HRR, Rad51 protein and its paralogues Rad52 and Rad54 have crucial roles. Studies using high doses of low LET radiation have identified additional accessory proteins that participate in DSB repair. Proteins involved in DSB repair have been grouped under three distinct categories: (i) damage sensors and mediators, (ii) signal transducers and (iii) effectors. Proteins belonging to the phosphatidylinositol-3 kinase (PI-3) super family, which are activated at very early stages of DNA damage induction, serve as sensors as well as the mediators of ensuing cellular repair and cell cycle checkpoint responses (1–5). PI-3 family members include Mec1p and Tel1p in the yeast *Saccharomyces cerevisiae*, Rad3 and Tel1 in *Schizosaccharomyces pombe* and ataxia telangiectasia mutated (ATM), ATM- and Rad3-related (ATR) and DNA-PK in humans. These proteins despite sharing a PI-3 kinase-like domain do not function as lipid kinases but serve as serine/threonine kinases. Among them, ATM, ATR and DNA-PK are critical for efficient cellular radio-responses as functional inactivation of these genes predisposes to hyper-radio sensitivity.

Bakkenist and Kastan (6) demonstrated that, inactive ATM dimeric molecules become active in response to DSB through autophosphorylation at serine 1981. The activated ATM monomers phosphorylate a number of downstream targets such as histone H2A variant, H2AX. A recent study has provided evidence for the phosphorylation of H2AX both by DNA-PK and ATM in a redundant, overlapping manner in mouse and human cells (7). This subsequently facilitates the recruitment and phosphorylation of other mediators such as mediator of DNA damage checkpoint protein 1 (MDC1), p53 binding protein 1 (53BP1), BRCA1 (breast cancer susceptibility gene) and Mre11-Rad50-Nbs1 complex. In case of replication-mediated DSB repair, ATR–ATR interacting protein complex is additionally recruited to the stalled replication forks by replication protein A (RPA). In a recent study, a time-dependent assembly of RPAp34 foci with γ -H2AX was demonstrated in response to DSB generated by both γ -rays and hydroxyurea (8). Nuclear foci formation by these multi-

protein mediator complexes promotes the transmission of DNA damage signal to downstream signal transducers such as Chk1, Chk2, Fanconi anaemia complementation group D2 (FANCD2) and structural maintenance of chromosome 1 (SMC1). Chk1 and Chk2 kinases phosphorylate downstream effectors like p53, CDC25A and CDC25C, leading to transient cell cycle delay to promote DSB repair. In case of excessive DNA damage, cell cycle checkpoint activation is prolonged, resulting in either senescence or apoptosis.

Much of our knowledge on induction and repair kinetics of DSB has come from studies performed at high doses of low and high LET radiations in 2D cell culture systems where each cell is traversed by many ionization events (9–13). However, our knowledge of DSB signalling and repair mechanisms in cells with 3D architecture that comprise the tissue microenvironment is highly restricted. Knowledge of tissue responses to radiation is an absolute requirement for estimating human health risks associated with chronic and acute doses of IR. With this objective, the present study was performed to analyse the radiation responses in 3D skin model system.

Methods

Cell culture and radiation treatment

Primary normal human lung fibroblasts (MRC5) were acquired from Coriell Cell Repository, Camden, NJ, USA. Fibroblast cells were routinely cultured essentially following the same procedure described previously (8,14,15). MRC5 cells in passage 12 were used for the present study. Human EpiDerm™ (skin model with only human primary keratinocytes) and EpiDermFT™ (full thickness skin model with both human primary keratinocytes and fibroblasts) tissue constructs were purchased from MatTek Corporation (Ashland, MA, USA). MRC5 cells and human EpiDerm tissue constructs (EpiDerm™ and EpiDermFT™) were irradiated with different doses of γ -rays (0.1–5 Gy) using a ^{137}Cs source delivering a dose rate of 0.82 Gy/min (Gamma Cell 40, Atomic Energy of Canada).

Immunological detection of DSB induction and repair in human cells

Immunological procedure for the detection of DSB markers [53BP1 (Novus Biologicals, Littleton, CO, USA), ATM^{ser1981}, DNA-PK^{T2609} and pan ATM/ATR (Cell Signaling Technology, Danvers, MA, USA)] was essentially the same as described earlier (8,14,15). 2D human fibroblasts in exponential growth phase were irradiated, incubated for various postrecovery time points (30 min, 2 h, 8 h, 24 h, 48 h and 72 h) and fixed in acetone:methanol (1:1). Tissue constructs, irradiated with different doses of γ -rays and postincubated for various time points, were fixed in buffered formalin and embedded in paraffin. Fixed paraffin sections were utilized for immunological detection of DSB induction and repair. The immunofluorescence procedure was carried out using the DAKO cytometry

kit (DAKO, Carpinteria, CA, USA). Briefly, the slides were washed in TBST (20 mM Tris-HCl pH 7.4, 137 mM NaCl and 0.2% Tween-20) and incubated for 30 min in TBST containing 5% NFDM (non-fat dried milk). The slides were washed in TBST and incubated with the primary and fluorochrome-conjugated secondary antibodies (1:100 dilution in TBST-5% NFDM) for 1 h at 37°C. The slides were washed in TBST, counter-stained for DNA either with propidium iodide (PI) or 4', 6-diamidino-2-phenylindole (DAPI, 0.1 µg/ml prepared in Vectashield mounting medium; Vector Laboratories, Burlingame, CA, USA.) and covered with a cover glass. The variously fluorochromed images were captured using a confocal laser scanning microscopy (Nikon, EZ.C1, Melville, NY, USA). For inhibition of PI-3 kinases, EpiDerm tissue constructs were treated with LY294002 (100 µM, EMD Biosciences, Gibbstown, NJ, USA) for 16 h prior to radiation treatment. Tissue sections were processed for immunofluorescence essentially as described above.

Quantitative analysis of IR-induced foci

Images of cells and EpiDerm tissue sections were captured from randomly selected fields using the confocal laser-scanning microscope. IR-induced foci as a function of radiation dose and postrecovery time were counted in the captured images both by eye and by Image J software (developed at the National Institutes of Health, Bethesda, MD, USA). Initially, nuclei were extracted by applying the threshold on DNA signal (DAPI or PI). For Image J software foci analysis, captured images were first converted to grey scale (16 bit) and a threshold was applied on fluorescein (488 nm) or Texas Red signal. For each nucleus, the number as well as the area of foci was measured. Image J software analysis yielded nearly similar foci number estimated by eye and the data from both types of analyses did not differ by more than 15%. At least 100 cells were scored for each radiation dose and postrecovery time and the data were pooled from two independent biological experiments. Results obtained on 53BP1 foci analysis are presented as XY scatter plot as a function of radiation dose and postrecovery time. Sham treated controls were included for all the postrecovery times and the basal level of 53BP1 foci number observed in sham treated fibroblasts and EpiDerm tissue constructs at different postrecovery times (30 min, 2 h, 8 h, 24 h, 48 h and 72 h) was subtracted from the IR-induced foci number in both cell model systems.

Detection of apoptotic cells by Apo-BrdU TUNEL assay

TUNEL assay was performed to determine the effects of high radiation doses on cell death in EpiDerm™ tissue constructs. EpiDerm™ tissue constructs were irradiated with different doses of γ-rays (2.5 and 5 Gy) and the irradiated tissues were incubated for different recovery times (24, 48 and 72 h). Tissues were fixed and processed essentially as described before. Paraffinized tissue sections were subjected to Apo-BrdU TUNEL assay (Invitrogen, Carlsbad, CA, USA) following the manufacturer's protocol (16). Cells were counterstained with PI. Apo-BrdU positive cells in randomly selected microscopic fields were scored. At least 200 cells were scored for each radiation dose and post-irradiation time.

Results

53BP1 is an efficient marker for the detection of DSB in human cells

The P53 binding protein 1 is recruited rapidly to DSB containing genomic DNA sites where they form distinct foci. To monitor DSB induction and repair, MRC5 cells were irradiated with low doses of γ -rays (0.1–0.5 Gy) and postincubated for various recovery times. In contrast to unirradiated cells, irradiated cells fixed 30 min after IR showed a dose-dependent increase in 53BP1 foci number in a non-linear fashion ([Fig. 1a](#)). A quantitative assessment of 53BP1 foci made in at least 100 randomly chosen cells is shown in [Fig. 1b](#). In this study, IR-induced foci number was estimated both by eye and Image J software (developed by NIH, Bethesda, MD). Comparative analyses of foci number estimated by both methods did not differ by more than 15% ([Fig. 1b](#)). In corroboration with earlier studies, 53BP1 foci induced by different doses of γ -rays radiation completely co-localized with that of γ -H2AX (data not shown). The average basal level of small residual 53BP1 foci was found to be 2.3 ± 0.31 per cell for human fibroblasts, 0.20 ± 0.04 for EpiDermTM and 0.24 ± 0.1 for EpiDermFTTM tissue constructs. The spontaneous 53BP1 foci number observed in sham treated primary fibroblasts and EpiDerm tissue constructs did not differ very much as a function of recovery time. The basal level of 53BP1 foci number observed in sham treated fibroblasts at 24, 48 and 72 h was found to be 2.27 ± 0.12 , 2.37 ± 0.12 and 2.26 ± 0.11 per cell, respectively. Similarly, the basal level of 53BP1 foci number in sham treated EpiDerm tissue constructs analysed at 24, 48 and 72 h was 0.25 ± 0.04 , 0.23 ± 0.06 and 0.26 ± 0.03 per cell, respectively. Unless otherwise stated, all the data presented on IR-induced foci number/cell for both fibroblasts and EpiDerm tissue constructs had the subtraction of background value of foci number observed in sham treated control cells at different recovery times. MRC5 cells irradiated with 0.1 Gy displayed 4.8 ± 0.4 foci/cell after 30 min of IR exposure. According to theoretical calculations, 0.1 Gy of low LET radiation should generate an average of 2.5 DSB (25 DSB/1 Gy) in the genomic DNA of a human diploid cell ([17](#)). A few studies have estimated the DSB number to be 40 in a human diploid cell after irradiation with 1 Gy of γ -rays ([18,19](#)). Thus, the number of 53BP1 foci observed after 0.1 Gy of γ -rays in our study correlates well with the expected number of DSB estimated by theoretical calculations. IR-induced 53BP1 foci number gradually declined with increasing post-irradiation times and a homogenous distribution of 53BP1 was observed by 24 h after IR in MRC5 cells irradiated with 0.1 Gy. Observation of complete disappearance of 53BP1 foci in cells irradiated with relatively low doses (0.1–0.5 Gy) after 24 h indicates that DSB repair occurs efficiently at low radiation doses. However, MRC5 cells irradiated with radiation doses higher than 1 Gy showed the persistence of 53BP1 foci in a dose-dependent manner. MRC5 cells irradiated with 0.5, 1 and 2.5 Gy showed a non-linear increase in 53BP1 and γ -H2AX foci after 30 min with increasing radiation doses (11.2 ± 0.8 foci/cell for 0.5 Gy, 19.2 ± 2.1 for 1 Gy and 51.7 ± 4.5 for 2.5 Gy of γ -rays). MRC5 cells irradiated with 2.5 and 5 Gy of γ -rays showed the persistence of five to six large 53BP1 and γ -H2AX foci per cell, respectively, for prolonged periods after radiation exposure (up to 72 h of analysis, data not shown).

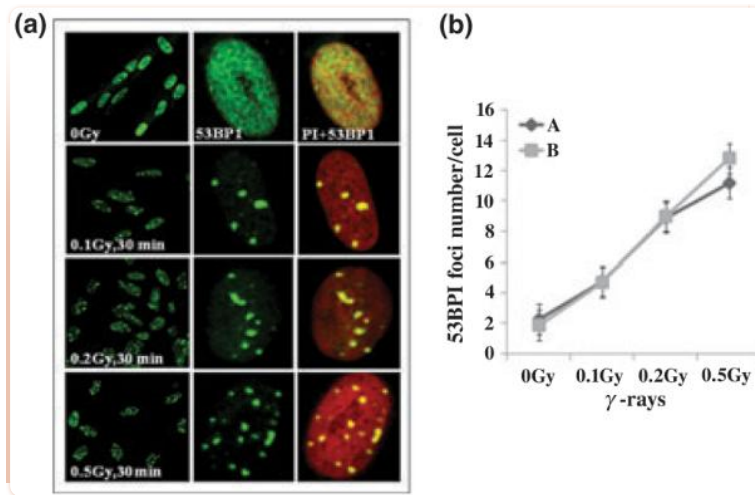


[Figure 1](#)

53BP1 is a sensitive marker for low-dose radiation-induced DSB in human cells. (a) Intra-nuclear assembly of γ -rays radiation-induced 53BP1 foci formation as a function of radiation dose in normal human primary fibroblast cells. MRC5 cells (in exponential growth phase) grown on two-well chamber slides were irradiated with varying doses of γ -rays and fixed after 30 min in acetone: methanol (1:1). Immunological detection of 53BP1 was performed using a primary antibody (Rabbit IgG, Novus Biologicals) and a fluorescein-conjugated secondary anti-rabbit antibody (Vector Laboratories). Cells were counterstained with propidium iodide. A microscopic field of cells observed for each γ -rays radiation dose is shown in the left most panels. (b) Quantitative assessment of radiation-induced 53BP1 foci number, as a function of radiation dose was determined in randomly chosen microscopic fields of cells by eye (a) and by Image J software (b). Bars represent the standard error of the mean. The background value of foci number observed in sham treated control cells was subtracted from IR-induced 53BP1 foci number.

Analysis of DSB induction and repair in human EpiDerm tissue constructs

An important component of this study, which is of special concern to US Department of Energy, is the determination of radiation-induced DNA damage responses in intact tissues or tissue-like constructs. Studies focused on elucidating the tissue-specific radiation responses are important for improving the accuracy of health risk estimation in intact human tissues. As 53BP1 efficiently forms foci at physiologically relevant low doses of IR, this approach was used to determine the DSB induction and repair responses in human skin constructs. In unirradiated tissues, 53BP1 was found to be more homogenous similar to that observed in 2D fibroblast cells. Upon irradiation, distinct focal sites of 53BP1 were observed in tissues as a function of radiation dose ([Fig. 2a](#)). The architecture of human EpiDerm™ tissue construct is shown by haematoxylin stained paraffinized tissue section ([Fig. 2b](#)). Upon irradiation with 0.1 Gy of γ -rays, an average of 3.0 ± 0.11 foci were induced 30 min after irradiation ([Fig. 2c](#)

). Analogous to that observed in human primary fibroblast cells, DSB repair, assessed by 53BP1 foci formation and disappearance, was found to be very efficient in tissues upon exposure to 0.1 Gy of γ -rays. However, tissues irradiated with 2.5 and 5 Gy of γ -rays showed the persistence of 53BP1 foci up to 72 h of analysis. Representative pictures showing the time course-kinetic analysis of 53BP1 foci formation observed in EpiDerm™ tissue constructs after 5 Gy of γ -rays is shown in [Fig. 3](#). The persistence of 53BP1 foci number increased with increasing radiation doses ([Fig. 4a](#)). As EpiDerm full thickness skin tissue model (EpiDermFT™) is very similar to human skin, time course kinetics of 53BP1 foci formation was next investigated in human EpiDermFT™ tissue constructs. The induction of DSB detected by 53BP1 foci formation in EpiDermFT™ tissue constructs after varying doses of γ -rays radiation was found to be similar to that observed in EpiDerm™ tissue constructs. Quantitative assessment of 53BP1 foci number performed in at least 100 randomly chosen cells as a function of radiation dose and postirradiation time in EpiDerm™ and EpiDermFT™ tissue constructs is shown in [Fig. 4a,b](#). Recruitment of phosphorylated ATM monomeric molecules to DSB sites was next investigated in conjunction with 53BP1. For this purpose, a combination of 53BP1 and ATM^{ser1981} antibodies was used. 53BP1 foci were found to precisely co-localize with phosphorylated ATM foci in the interphase nuclei after γ -rays radiation in both types of EpiDerm tissue constructs. Further, the time course kinetics of phosphorylated ATM foci formation as a function of recovery time after γ -rays was found to be very similar to 53BP1.

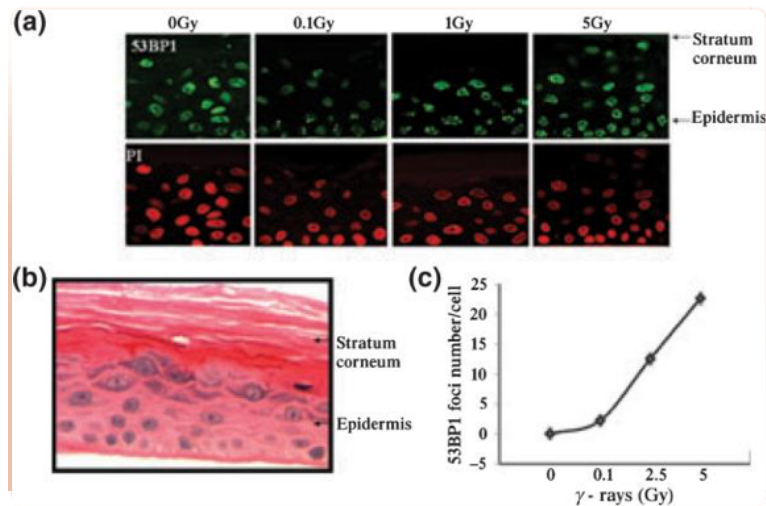


[Figure 2](#)

Detection of DSB induction in human 3D EpiDerm™ tissue constructs. (a) Immunological analysis of DSB induction as a function of radiation dose in human 3D EpiDerm tissue constructs. EpiDerm™ tissue constructs were irradiated with indicated doses of γ -rays and fixed 30 min after treatment in buffered formalin. Paraffinized tissue sections were used for immunological detection of 53BP1 using fluorescein conjugated secondary antibody. Cells were counterstained with propidium iodide. (b) Paraffinized haematoxylin stained tissue section showing the architecture of 3D tissue constructs. (c) Quantitative assessment of 53BP1 foci induced by different γ -rays radiation doses in at least 100 randomly chosen cells for each radiation dose. Bars represent the standard error of the mean.

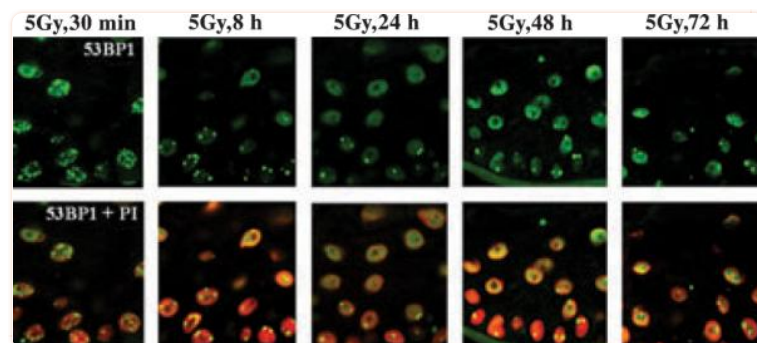


[Figure 3](#)

EpiDerm™ tissue constructs irradiated with high doses of γ -rays showed persistence of 53BP1 foci. EpiDerm tissue constructs were irradiated with 5 Gy of γ -rays and fixed at different post recovery time points. Cells were counterstained with propidium iodide.

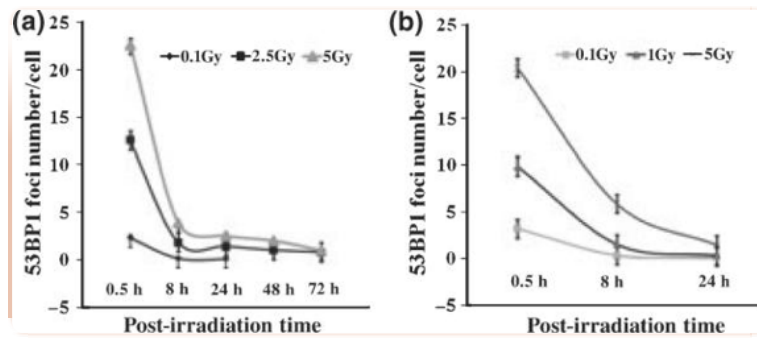


[Figure 4](#)

Quantitative assessment of DSB induction and repair as a function of radiation dose and recovery time in human EpiDerm™ (a) and EpiDermFT™ (b) tissue constructs. Data obtained on the time course kinetics of foci formation and persistence after different radiation doses and post-irradiation times are presented as a XY-scatter plot.

It is interesting to note that the basal layer of cells in EpiDerm tissue constructs showed efficient 53BP1 foci formation, whereas the 53BP1 foci formation was hardly detectable in cells proximal to stratum corneum ([Fig. 2a](#)). It is known that cells proximal to stratum corneum in human skin contain excessive amounts of keratin and some of these cells may not be viable. To verify this, human EpiDerm™ and EpiDermFT™ tissue sections were immunostained with an antibody specific for human epidermal keratins (ABR Affinity BioReagents, Rockford, IL, USA). This antibody recognizes cytokeratins of acidic (10, 14, 15, 16, and 19) and basic families (1, 2, 3, 4, 5, 6 and 8). As expected, intense cytoplasmic staining of keratins was observed in cells that were proximal to stratum corneum (data not shown).

Analysis of apoptotic cell death by Apo-BrdU TUNEL assay

If cells with persistent 53BP1 foci represent irreparable DSB or misrepaired DSB, such cells are likely to undergo apoptosis through accumulation of genomic instability. To verify this, frequency of apoptotic cells was estimated in EpiDerm™ tissue constructs irradiated with 2.5 and 5 Gy of γ -rays. For this purpose, an Apo-BrdU-based TUNEL assay was performed. In addition, the percentage of cells with persistent 53BP1 foci was also determined after different post-irradiation times (24, 48 and 72 h). The results seem to suggest that the apoptotic death induced by high radiation doses may be due to either irreparable DSB or misrepaired DSB ([Fig. 5a,b](#)).

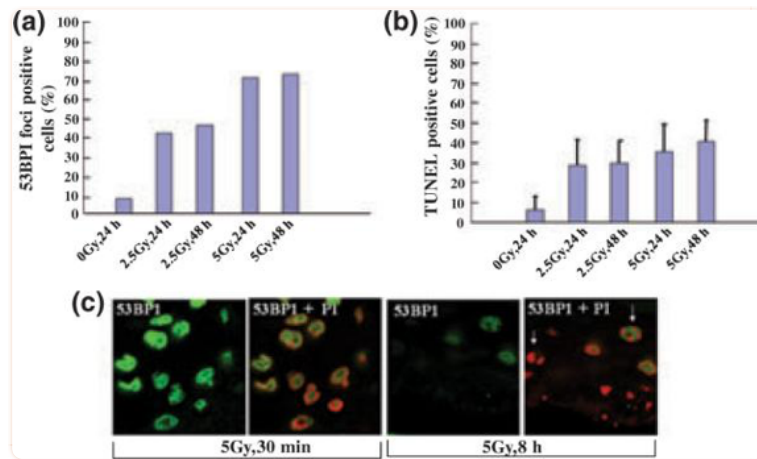


[Figure 5](#)

Analysis of IR-induced apoptotic cell death in human EpiDerm™ tissue constructs by Apo-BrdU TUNEL assay. (a) Percentage of 53BP1 foci positive cells observed at 24 and 48 h after 2.5 and 5 Gy of γ -rays radiation. (b) The frequency of apoptotic cells determined by Apo-BrdU TUNEL assay as a function of radiation dose and recovery time. Bars indicate the standard deviation of the mean. At least 200 cells were scored for each radiation dose and recovery time. (c) Abolition of PI-3 kinases inhibits 53BP1 foci formation and causes apoptosis in human EpiDerm™ tissue constructs. EpiDerm™ tissue constructs were treated with LY294002 prior to radiation treatment with 5 Gy of γ -rays. Tissue sections were fixed after different postincubation time points (30 min, 8 h and 24 h). Tissue sections were immunostained using 53BP1 primary antibody and fluorescein conjugated secondary antibody. Arrows indicate the apoptotic cells with fragmented chromatin bodies.

PI-3 kinase inhibitor abolishes 53BP1 foci formation and causes apoptotic death in EpiDerm tissue constructs

We have demonstrated an efficient induction of intra-nuclear foci formation by PIKK involving ATM, ATR and DNA-PK as a function of radiation dose in 3D human tissue constructs. These observations demonstrate the existence of efficient DSB-mediated signalling pathways in tissues. In order to verify whether PI-3K- and PIKK-mediated signal transduction pathways are important for DSB recognition and repair in tissue microenvironment, EpiDerm™ tissues were treated with a PI-3K and PIKK inhibitor LY294002 at a concentration of 100 μ M prior to radiation exposure. Treatment of PI-3 kinase inhibitor completely abolished 53BP1 foci formation and resulted in apoptotic death of the cells ([Fig. 5c](#)). This clearly illustrates the importance of PIKK-mediated signalling pathways for DSB recognition and repair of DSB in tissues. Currently, experiments using commercially available specific and potent inhibitors for ATM, ATR and DNA-PK are in progress to evaluate the effects of low doses of low LET radiation in tissue constructs.

Discussion

Knowledge of DNA damage responses in cells with 3D architecture in tissue microenvironment is highly restricted. With this objective, the present study was carried out to investigate the radio responses in human 3D tissue microenvironment. This information is critical for the accurate prediction of radiation-induced health risks in humans. The present study compared the radiation responses between 2D human fibroblasts and 3D human skin tissue constructs with special emphasis on the detection of DSB induction and repair. Although skin is not the most radio-sensitive organ, we chose EpiDerm tissue constructs for our study because this model system has been very well characterized and extensively used by several laboratories. Human skin model systems (EpiDerm™ and EpiDermFT™) used in this study exhibit *in vivo-like* morphological and growth characteristics, which are uniform and highly reproducible. This artificial skin model is widely used by several laboratories because EpiDerm skin model consists of organized basal, spinous, and granular, and cornified layers analogous to those found *in vivo*.

For achieving the goal of this study, we wished to determine IR-induced DSB induction and repair *in situ* without disrupting the architecture of 3D human tissue microenvironment. An immunological *in situ* approach was therefore undertaken to monitor IR-induced DNA damage and repair.

Earlier studies have demonstrated that histone H2A variant H2AX, rapidly phosphorylated by PI-3 kinase like kinases (PIKK), is recruited to DSB sites (20,21). Additionally, two other sensor proteins, 53BP1 and MDC1, also accumulate at DSB sites in response to IR, although the precise sequence of assembly of these proteins is not known (22–26). 53BP1 physically interacts with a number of proteins that have demonstrated roles in DSB repair. Earlier studies have provided suggestive evidence for a role of 53BP1 in DSB repair (27–31). Owing to its importance in DSB repair, we have chosen 53BP1 to monitor DSB induction and repair in human skin model system.

Using the immunological approach, DSB induction and repair has been successfully demonstrated for the first time in 3D EpiDerm tissue constructs. Both 53BP1 foci number and 53BP1 foci positive cells analysed at 30 min after IR exposure showed a non-linear increase with increasing doses of γ -rays in both human fibroblasts and EpiDerm tissue constructs. Two distinct differences were observed between 2D (human fibroblasts) and 3D (EpiDerm™ and EpiDermFT™ tissue constructs) model systems: (i) 53BP1 foci were fewer in EpiDerm tissue constructs and (ii) heterogeneity in the distribution of 53BP1 foci was observed among different cell layers of EpiDerm tissue constructs. The reason for fewer number of 53BP1 foci formed in the EpiDerm tissue constructs is not fully understood at the moment. We speculate that the scattering of γ -rays radiation by the stratum corneum may be responsible for the less number of 53BP1 foci observed in the basal cells in EpiDerm tissue constructs. A recent study has demonstrated that that IR-induced foci were detected readily in

the less DNA dense regions as opposed to highly condensed heterochromatic regions suggestive of the influence of chromatin organization on IR-induced foci formation (32). Further studies are required to determine the basis for the reduced number of 53BP1 foci observed in keratinocytes after radiation exposure.

Unlike dermal fibroblasts which did not show any heterogeneity in 53BP1 foci formation, IR-induced 53BP1 foci were predominantly found in the basal layer of cells in tissue constructs while cells proximal to stratum corneum failed to show any 53BP1 foci in EpiDerm constructs. It is known that the cells proximal to stratum corneum in human skin contain excessive amounts of keratin and some of these cells are not viable. Although variations in IR-induced 53BP1 foci number were observed between primary human fibroblasts and EpiDerm tissue constructs, DSB repair was found to be efficient in both cell systems at low doses of γ -rays.

Persistence of 53BP1 foci was observed both in human fibroblasts and EpiDerm tissue constructs irradiated with high doses of γ -rays (2.5 and 5 Gy) for prolonged periods of analysis (up to 72 h after IR exposure). In contrast, persistence of 53BP1 foci was not observed in both cell model systems at radiation doses ranging from 10 cGy to 1Gy of γ -rays. Assuming that the persistent 53BP1 foci reflect irreparable/misrepaired DSB, one would predict that such cells would eventually undergo mitotic catastrophe and apoptosis. To verify this notion, frequency of apoptotic cells induced by high radiation doses (2.5 and 5 Gy of γ -rays) was measured by Apo-BrdU TUNEL assay after 24, 48 and 72 h of radiation exposure in human skin tissue constructs. The results showed a positive correlation between the percentage of cells with persistent 53BP1 foci and the apoptotic cells. In corroboration with our results, a recent study has reported X-ray-induced apoptosis in human keratinocytes and the apoptosis occurs in a protein kinase C delta-dependent manner (33). Analogous to 53BP1 foci, persistence of foci detected by ATM/ATR-specific pan antibody was also observed in tissue constructs irradiated with high doses (2.5 and 5 Gy) of γ -rays.

In this study, we demonstrated that pretreatment of EpiDerm tissue constructs with a PI-3 kinase inhibitor (LY294002) not only abolished IR-induced 53BP1 foci formation but also resulted in apoptosis. Abolition of IR-induced 53BP1 foci formation is probably because of the inhibition of the activities of PIKK involving ATM, ATR and DNA-PK. Consistent with this notion, Lee et al. (34) demonstrated that the phosphorylation of 53BP1 at ser¹²¹⁹ by ATM kinase is critical for an efficient DNA damage response and suppression of 53BP1 phosphorylation at this site also impairs the recruitment of other DNA damage sensing molecules such as γ -H2AX and MDC1 to DSB sites. DiTullio et al. (28) demonstrated that 53BP1 functions as a DNA damage checkpoint protein and 53BP1 is required at least for a subset of ATM-dependent downstream phosphorylation events. These studies clearly illustrate the critical requirement of 53BP1 in IR-induced DNA damage response. Therefore, the increased apoptotic death observed after treatment with PI-3 kinase inhibitor in EpiDerm tissue constructs is probably because of disruption of efficient DNA damage response as evidenced by the abolition of 53BP1 foci formation.

In summary, we have successfully demonstrated the feasibility of monitoring the induction and repair of DSB induced by low and high doses of low LET radiation in human tissue constructs. Our study demonstrates the existence of an efficient PIKK-mediated DSB repair machinery in human EpiDerm tissue constructs. This model system can be effectively used for assessing the biological effects of IR in a tissue microenvironment.

Acknowledgements

We appreciate the help of Dr Peter Grabham with Image J software analysis. This study was financially supported by research grants from US Department of Energy, Office of Sciences (BER) awarded to A. S. Balajee (DE-FG02-05ER64055) and C. R. Geard (DE-FG02-05ER64054). A. S. Balajee and C. R. Geard acknowledge the financial support received from NIH/NCI (5P01CA49062-17). The pilot and feasibility grant to A. S. Balajee (NIH-NIAMS, P30) received from Skin Disease Research Center, Department of Dermatology, Columbia University Medical Center, NY is gratefully acknowledged.

References

1. Durocher D, Jackson SP. DNA-PK, ATM and ATR as sensors of DNA damage: variations on a theme? *Curr Opin Cell Biol.* 2001;13:225–231. [[PubMed](#)] [[Google Scholar](#)]
2. Kinner A, Wu W, Staudt C, Iliakis G. Gamma-H2AX in recognition and signaling of DNA double-strand breaks in the context of chromatin. *Nucleic Acids Res.* 2008;36:5678–5694. [[PMC free article](#)] [[PubMed](#)] [[Google Scholar](#)]
3. Kobayashi J, Iwabuchi K, Miyagawa K, et al. Current topics in DNA double-strand break repair. *J Radiat Res (Tokyo)* 2008;49:93–103. [[PubMed](#)] [[Google Scholar](#)]
4. Riches LC, Lynch AM, Gooderham NJ. Early events in the mammalian response to DNA double-strand breaks. *Mutagenesis.* 2008;23:331–339. [[PubMed](#)] [[Google Scholar](#)]
5. Shiloh Y. ATM and related protein kinases: safeguarding genome integrity. *Nat Rev Cancer.* 2003;3:155–168. [[PubMed](#)] [[Google Scholar](#)]
6. Bakkenist CJ, Kastan MB. DNA damage activates ATM through intermolecular autophosphorylation and dimer dissociation. *Nature.* 2003;421:499–506. [[PubMed](#)] [[Google Scholar](#)]
7. Stiff T, O'Driscoll M, Rief N, Iwabuchi K, Lobrich M, Jeggo PA. ATM and DNA-PK function redundantly to phosphorylate H2AX after exposure to ionizing radiation. *Cancer Res.* 2004;64:2390–2396. [[PubMed](#)] [[Google Scholar](#)]
8. Balajee AS, Geard CR. Replication protein A and gamma-H2AX foci assembly is triggered by cellular response to DNA double-strand breaks. *Exp Cell Res.* 2004;300:320–334. [[PubMed](#)] [[Google Scholar](#)]

9. Bassing CH, Alt FW. H2AX may function as an anchor to hold broken chromosomal DNA ends in close proximity. *Cell Cycle*. 2004;3:149–153. [[PubMed](#)] [[Google Scholar](#)]
10. Bassing CH, Alt FW. The cellular response to general and programmed DNA double strand breaks. *DNA Repair (Amst)* 2004;3:781–796. [[PubMed](#)] [[Google Scholar](#)]
11. Jackson SP. Sensing and repairing DNA double-strand breaks. *Carcinogenesis*. 2002;23:687–696. [[PubMed](#)] [[Google Scholar](#)]
12. Thacker J, Zdzienicka MZ. The XRCC genes: expanding roles in DNA double-strand break repair. *DNA Repair (Amst)* 2004;3:1081–1090. [[PubMed](#)] [[Google Scholar](#)]
13. Thompson LH, Schild D. Recombinational DNA repair and human disease. *Mutat Res*. 2002;509:49–78. [[PubMed](#)] [[Google Scholar](#)]
14. Balajee AS, Geard CR. Chromatin-bound PCNA complex formation triggered by DNA damage occurs independent of the ATM gene product in human cells. *Nucleic Acids Res*. 2001;29:1341–1351. [[PMC free article](#)] [[PubMed](#)] [[Google Scholar](#)]
15. Li H, Balajee AS, Su T, Cen B, Hei TK, Weinstein IB. The HINT1 tumor suppressor regulates both gamma-H2AX and ATM in response to DNA damage. *J Cell Biol*. 2008;183:253–265. [[PMC free article](#)] [[PubMed](#)] [[Google Scholar](#)]
16. Meador JA, Zhao M, Su Y, Narayan G, Geard CR, Balajee AS. Histone H2AX is a critical factor for cellular protection against DNA alkylating agents. *Oncogene*. 2008;27:5662–5671. [[PubMed](#)] [[Google Scholar](#)]
17. Stenerlow B, Karlsson KH, Cooper B, Rydberg B. Measurement of prompt DNA double-strand breaks in mammalian cells without including heat-labile sites: results for cells deficient in nonhomologous end joining. *Radiat Res*. 2003;159:502–510. [[PubMed](#)] [[Google Scholar](#)]
18. Cedervall B, Radivoyevitch T. Methods for analysis of DNA fragment distributions on pulsed field gel electrophoretic gels. *Electrophoresis*. 1996;17:1080–1086. [[PubMed](#)] [[Google Scholar](#)]
19. Ruiz de Almodovar JM, Steel GG, Whitaker SJ, McMillan TJ. A comparison of methods for calculating DNA double-strand break induction frequency in mammalian cells by pulsed-field gel electrophoresis. *Int J Radiat Biol*. 1994;65:641–649. [[PubMed](#)] [[Google Scholar](#)]
20. Rogakou EP, Boon C, Redon C, Bonner WM. Megabase chromatin domains involved in DNA double-strand breaks in vivo. *J Cell Biol*. 1999;146:905–916. [[PMC free article](#)] [[PubMed](#)] [[Google Scholar](#)]
21. Rogakou EP, Pilch DR, Orr AH, Ivanova VS, Bonner WM. DNA double-stranded breaks induce histone H2AX phosphorylation on serine 139. *J Biol Chem*. 1998;273:5858–5868. [[PubMed](#)] [[Google Scholar](#)]
22. Anderson L, Henderson C, Adachi Y. Phosphorylation and rapid relocalization of 53BP1 to nuclear foci upon DNA damage. *Mol Cell Biol*. 2001;21:1719–1729. [[PMC free article](#)] [[PubMed](#)] [[Google Scholar](#)]
23. Goldberg M, Stucki M, Falck J, et al. MDC1 is required for the intra-S-phase DNA damage checkpoint. *Nature*. 2003;421:952–956. [[PubMed](#)] [[Google Scholar](#)]

24. Rappold I, Iwabuchi K, Date T, Chen J. Tumor suppressor p53 binding protein 1 (53BP1) is involved in DNA damage-signaling pathways. *J Cell Biol.* 2001;153:613–620. [[PMC free article](#)] [[PubMed](#)] [[Google Scholar](#)]
25. Schultz LB, Chehab NH, Malikzay A, Halazonetis TD. p53 binding protein 1 (53BP1) is an early participant in the cellular response to DNA double-strand breaks. *J Cell Biol.* 2000;151:1381–1390. [[PMC free article](#)] [[PubMed](#)] [[Google Scholar](#)]
26. Stewart GS, Wang B, Bignell CR, Taylor AM, Elledge SJ. MDC1 is a mediator of the mammalian DNA damage checkpoint. *Nature.* 2003;421:961–966. [[PubMed](#)] [[Google Scholar](#)]
27. Adams MM, Carpenter PB. Tying the loose ends together in DNA double strand break repair with 53BP1. *Cell Div.* 2006;1:19. [[PMC free article](#)] [[PubMed](#)] [[Google Scholar](#)]
28. DiTullio RA, Jr, Mochan TA, Venere M, et al. 53BP1 functions in an ATM-dependent checkpoint pathway that is constitutively activated in human cancer. *Nat Cell Biol.* 2002;4:998–1002. [[PubMed](#)] [[Google Scholar](#)]
29. Fernandez-Capetillo O, Chen HT, Celeste A, et al. DNA damage-induced G2-M checkpoint activation by histone H2AX and 53BP1. *Nat Cell Biol.* 2002;4:993–997. [[PubMed](#)] [[Google Scholar](#)]
30. Ward IM, Minn K, Jorda KG, Chen J. Accumulation of checkpoint protein 53BP1 at DNA breaks involves its binding to phosphorylated histone H2AX. *J Biol Chem.* 2003;278:19579–19582. [[PubMed](#)] [[Google Scholar](#)]
31. Ward IM, Minn K, van Deursen J, Chen J. p53 Binding protein 53BP1 is required for DNA damage responses and tumor suppression in mice. *Mol Cell Biol.* 2003;23:2556–2563. [[PMC free article](#)] [[PubMed](#)] [[Google Scholar](#)]
32. Costes SV, Ponomarev A, Chen JL, Nguyen D, Cucinotta FA, Barcellos-Hoff MH. Image-based modeling reveals dynamic redistribution of DNA damage into nuclear sub-domains. *PLoS Comput Biol.* 2007;3:e155. [[PMC free article](#)] [[PubMed](#)] [[Google Scholar](#)]
33. Lee YS, Sohn KC, Kim KH, et al. Role of protein kinase C delta in X-ray-induced apoptosis of keratinocyte. *Exp Dermatol.* 2009;18:50–56. [[PubMed](#)] [[Google Scholar](#)]
34. Lee H, Kwak HJ, Cho IT, Park SH, Lee CH. S1219 residue of 53BP1 is phosphorylated by ATM kinase upon DNA damage and required for proper execution of DNA damage response. *Biochem Biophys Res Commun.* 2009;378:32–36. [[PubMed](#)] [[Google Scholar](#)]

